NUCLEAR PHOTO-SCIENCE AND APPLICATIONS WITH THOMSON-RADIATED EXTREME X-RAY (T-REX) SOURCES*

F.V. Hartemann, S.G. Anderson, S.M. Betts, D.J. Gibson, E.P. Hartouni, I. Jovanovic, A.K. Kerman[†], M. Messerly, D.P. McNabb, J. Pruet, J. Rosenzweig[‡], M.Y. Shverdin, C.W. Siders, A.M. Tremaine, and C.P.J. Barty[#], LLNL, Livermore, CA 94550, U.S.A.

Abstract

Recent advances in high brightness rf gun technology, coupled with novel laser systems and architecture have enabled the development of a new class of compact, tunable, monochromatic light sources capable of producing MeV photons with unprecedented brightness. Such new sources rely on Thomson scattering of incident photons produced by a TW-class laser off a bright relativistic electron beam to generate Doppler-upshifted photons in a highly collimated beam. Scaling laws [1] show that a frequency-doubled, 532 nm wavelength, 1 J, 10 ps Fourier transform-limited drive laser pulse interacting with a 250 MeV, 1 nC, 10 ps, 1 mm.mrad normalized emittance, with 0.1% relative energy spread, can yield a 2.24 MeV γ-ray flash with a peak brightness exceeding 10^{23} photons/[mm^2 x mrad^2 x s x 0.1% bandwidth]. This number is > 15 orders of magnitude beyond the output of a third-generation synchrotron at the same photon energy. Above ~ 100 keV, the photons can interact with nuclei, and nuclear applications become viable. In this paper, we present a technical overview of T-REX sources and their capabilities, and give a few examples of potential applications of interest.

INTRODUCTION

Recent advances in high brightness rf gun and fiber laser technology have enabled the development of a new class of compact, tunable, narrow-bandwidth light sources capable of producing MeV photons with unprecedented brightness. Such new sources rely on Thomson scattering of incident photons produced by a TW-class laser off a bright relativistic electron beam to generate Doppler-upshifted photons in a highly collimated beam. The main goal of this paper is to present a technical overview of so-called T-REX (Thomson-radiated extreme x-ray) sources and their key capabilities, and to provide a few examples of potential applications of particular interest.

This paper is organized as follows: a brief theoretical overview of Compton scattering and its salient features is first presented; the key rf gun and laser enabling technologies are then cursorily described; finally, a few important nuclear applications are outlined.

We note that, while we typically use the Thomson scattering terminology in this paper, the process is, strictly speaking, Compton scattering in the low recoil limit.

* This work was performed under the auspices of the U.S. Department of Energy by University of California, Lawrence Livermore National Laboratory under Contract W-7405-Eng-48.

[†] MIT, Cambridge, MA 02139, U.S.A.
[‡] UCLA, Los Angeles, CA 60439, U.S.A.
[#]barty1@llnl.gov

COMPTON SCATTERING

Incident photons, with 4-wavenumber $k_\mu = (\omega_0 / c, \mathbf{k}_0)$, can Compton scatter off electrons with initial 4-momentum $m_0 c u_\mu$, to be Doppler-upshifted according to the Compton formula, which is derived from 4-momentum conservation: $\hbar k_\mu + m_0 c u_\mu = \hbar q_\mu + m_0 c v_\mu$, where q_μ is the 4-wavenuber of the scattered photon, and $m_0 c v_\mu$ is the electron 4-momentum after the interaction. Using the dispersion relation in vacuum, $k_\mu k^\mu = 0$, and the relation between energy and momentum, $u_\mu u^\mu = \gamma^2 - \mathbf{u}^2 = 1$, one obtains the Compton formula:

$$\omega_x = \frac{\gamma\omega_0 - \mathbf{u}\cdot c\mathbf{k}_0}{\gamma + \lambda\!\!\!^{-}_C k_0 - \mathbf{n}_x \cdot \left(\mathbf{u} + \lambda\!\!\!^{-}_C \mathbf{k}_0\right)}. \quad (1)$$

Here, ω_x is the frequency of the scattered photon, and $\mathbf{n}_x$ is a unit vector in the direction of observation; $\lambda\!\!\!^{-}_C = \hbar / m_0 c$ is the Compton wavelength of the electron.

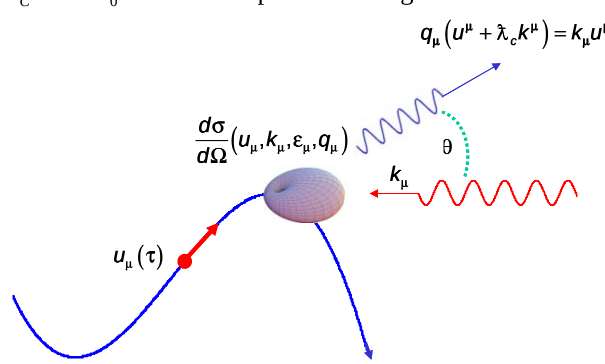

Figure 1: Schematic of Compton scattering.

Neglecting recoil and considering head-on collisions, Eq. (1) takes the familiar form:

$$\frac{\omega_x}{\omega_0} = \frac{\gamma + u}{\gamma - u\cos\theta}, \quad (2)$$

where θ is the scattering angle, as illustrated in Fig. 1; this leads to a full Doppler upshift of $4\gamma^2$ in the case of on-axis radiation, where $\theta = 0$.

The differential cross-section for this process is described by the Lorentz-boosted Klein-Nishina formula [2],

$$\frac{d\sigma}{d\Omega_x} = \frac{r_0^2}{2}\left(\frac{\omega_x}{\kappa_0}\right)^2 \left\{ \begin{array}{l} \frac{1}{2}\left(\frac{\kappa_0}{\kappa_x}+\frac{\kappa_x}{\kappa_0}\right)-1 \\ +2\left[\begin{array}{l} \varepsilon_\mu^0 \varepsilon_x^\mu - \frac{\left(\varepsilon_\mu^0 u^\mu\right)\left(\varepsilon_\mu^x v^\mu\right)}{\kappa_0} \\ -\frac{\left(\varepsilon_\mu^x u^\mu\right)\left(\varepsilon_\mu^0 v^\mu\right)}{\kappa_x} \end{array} \right]^2 \end{array} \right\}. \quad (3)$$

Here we have limited the expression for the cross-section to spin-unpolarized electron beams; r_0 is the classical electron radius; $\kappa_0 = u_\mu k^\mu$ and $\kappa_x = v_\mu q^\mu$ are the incident and scattered light-cone variables; finally, ε_μ^0 and ε_μ^x are the incident and scattered 4-polarizations. The differential cross-section integrates to the well-known Thomson cross-section, $\sigma = 8\pi r_0^2/3$.

The brightness of Thomson scattering light sources was been studied theoretically [1] and computationally [3], and shown to scale favorably at high energy; this is due to the close correlation between the scattered light phase space and that of the incident electron beam: for a given normalized emittance, ε_n, the physical emittance of the electron beam scales as ε_n/γ; in turn, this implies that the scattered light is better collimated and has narrower bandwidth. For example, given the laser and electron beam parameters described in Table 1, the peak on-axis spectral brightness is shown in Fig. 2: the blue line corresponds to the analytical theory presented in Ref. [1], while the red squares are generated by a fully three-dimensional code that has been extensively benchmarked against a series of detailed experiments at LLNL [3]; the maximum brightness is shown to scale as $(\gamma/\varepsilon_n)^2$.

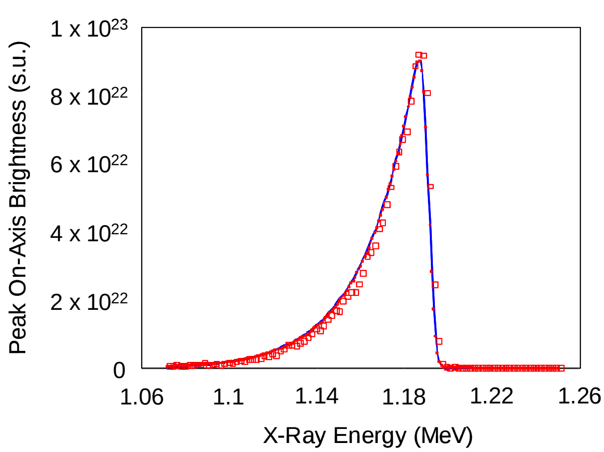

Figure 2: On-axis spectral brightness.

LLNL T-REX SOURCE

A prototype T-REX source is currently under construction at LLNL; it has been designed to perform proof-of-principle nuclear resonance fluorescence (NRF) imaging experiments at photon energies up to 700 keV. The overall system architecture is shown in Fig. 3; key components include a high brightness S-band rf gun and associated fiber-based UV photocathode laser system, a 125 MeV linac, and a Joule-class, 10 Hz drive laser, with frequency tripling down to 355 nm. This source will produce 10^9 photons/shot; the effective γ-ray beam divergence will be 0.5 mrad; and its fractional bandwidth will be < 5%.

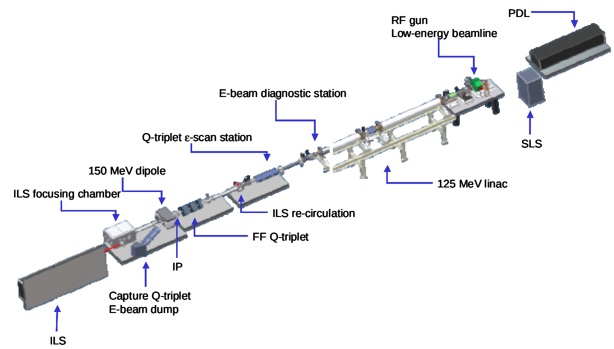

Figure 3: T-REX overall schematic.

Table 1: Linac and Laser Parameters

	Linac	Laser
Particle energy	50 MeV	$\hbar\omega_0 = 1.24$ eV
Particle #	$q = N_e e = 1$ nC	$W = 1$ J
Pulse duration	$\Delta\tau/\sqrt{2} = 100$ fs	$\Delta t = 5$ ps
Focal spot radius	$r_b/\sqrt{2} = 10$ μm	$w_0 = 20$ μm
Energy spread	$\Delta\gamma/\sqrt{2}\gamma = 0.1\%$	$\Delta\omega = \sqrt{2}/\Delta t$
Transverse phase space (*rms*)	$\varepsilon_n = 1$ mm.mrad	$\Delta k_\perp / k_0 \ll 1$

As indicated in the previous section, the x-ray phase space closely maps that of the electron beam; this implies that high charge, low emittance and low energy spread electron beams are critical to enable the development of high brightness Thomson scattering light sources. Additional issues, such as the picosecond timing required between the electron and laser beams, also point in the direction of rf guns as the electron source of choice.

One of the key characteristics of rf guns is the very high accelerating gradient under which the system operates: up to 120 MeV/m for good vacuum and processing conditions. This yields very bright photo-electron bunches that are naturally synchronized to the laser pulses used to illuminate the photocathode. However, to take full advantage of the unique properties of rf guns, one requires highly specific spatial and temporal laser pulse shapes at the photocathode. Namely, two possible schemes can be envisioned: for high-charge (~ 1 nC) operation at S-band, a nearly uniform density, ~ 10 ps, spatio-temporally cylindrical laser pulse is required; for lower charge applications (~ 100 pC) a uniform density, ~ 100 fs, spatio-temporally ellipsoidal laser pulse represents the best profile, as it translates into linear space-charge forces in the electron bunch [4]. Each approach is very demanding for the photocathode drive laser, even though sputtered Mg can reduce the UV laser requirement down to a few tens or a few hundreds of μJ.

In addition, the design of the rf gun requires careful planning in order to achieve the aforementioned accelerating gradients, which are key to the gun performance; these include the proper separation between the π an 0-modes, the proper field balance between cells, measures aiming at reducing the potential for arcing, and detailed implementation of emittance compensation. For illustration, a schematic of the new UCLA/LLNL gun is shown in Fig. 4.

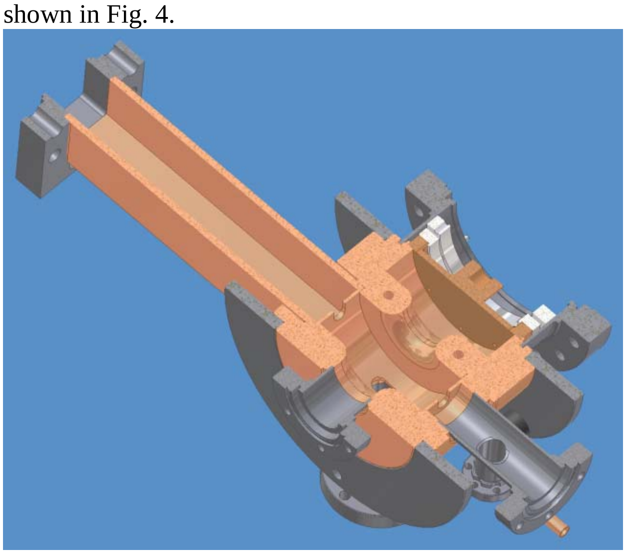

Figure 4: UCLA/LLNL S-band rf gun.

Given the stringent laser requirements for both the Thomson scattering drive laser and the rf gun photocathode illumination system, and the need for robustness, compactness, efficiency, and versatility, fiber-based systems appear to be ideal candidates to meet the technical specifications of Thomson light sources. Such novel lasers are highly stable, in part because of diode pumping; integrated optics, including fiber switches and chirped fiber Bragg gratings allow for the production and manipulation of ultrashort laser pulses, with energies up to 1 mJ. Higher energies can be obtained by bulk amplification, while the fiber systems themselves are readily scaleable to multi-kW average powers.

Using hyper-Michelson interferometers [5], it is possible to produce arbitrary and well-defined UV pulses.

APPLICATIONS

The unique properties of T-REX light sources will enable and spur new applications in the nuclear photonics regime, taking advantage of their intrinsic brightness, tunability, narrow bandwidth, low divergence, and small source size. For example, the scattered radiation can be fully polarized, thus allowing for parity experiments similar to those performed at HIGS [6]. Further, methods to bring the bandwidth well below 10^{-4} are under study.

Nuclear Resonance Fluorescence & Imaging

Under irradiation by high energy photons, nuclei can exhibit sharp resonances, corresponding to various modes of oscillation of the charge distribution in the nucleus. The precise frequency of these resonances depends not only on the atomic number of the nucleus under investigation, but also on its particular isotope. In addition, these high energy resonances have large cross-sections, and can be found in an energy range where materials are highly transparent. These unique physical properties open a path to isotopic imaging of bulk materials, with direct implications for Homeland Security, as articulated technically in Ref. [7].

One of the grand challenges in x-ray imaging is the detection of low-Z, low density materials behind high-Z, high density shielding. One can take advantage of the NRF technique outlined above, and illuminate the system under inspection on resonance for the light material, at an energy where the shielding does not present significant absorption.

Nuclear Waste Transmutation

Finally, it is noteworthy that T-REX sources can, in principle, be scaled to γ-ray outputs in excess of 10 kW cw, using energy-recovery linacs, ceramic-based lasers, and advanced coherent aperture phasing techniques; such sources offer an alternative path to nuclear waste transmutation via direct photon-nuclei interactions.

REFERENCES

[1] F.V. Hartemann, *et al.*, “High-energy scaling of Compton scattering light sources”, Phys. Rev. STAB **8**, 100702 (2005).

[2] G. Bhatt, *et al.*, “Relativistic spin-dependent Compton scattering from electrons”, Phys. Rev. **A28**, 2195 (1983).

[3] W.J. Brown, *et al.*, “Three-dimensional time and frequency-domain theory of femtosecond x-ray pulse generation through Thomson scattering”, Phys. Rev. STAB **7**, 060702; “Experimental characterization of an ultrafast Thomson scattering x-ray source”, *ibid* 060703 (2004).

[4] O.J. Luiten, *et al.*, “How to realize uniform three-dimensional ellipsoidal electron bunches”, Phys. Rev. Lett. **93**, 094802 (2004).

[5] C.W. Siders, *et al.*, “Efficient high-energy pulse-train generation using a 2n-pulse Michelson interferometer”, Appl. Opt. **37**, 5302 (1998).

[6] N. Pietralla and Z. Berant, “Parity measurements of nuclear levels using a free-electron-laser generated γ-ray beam”, Phys. Rev. Lett. **88**, 012502 (2001).

[7] J. Pruet, *et al.*, “Detecting clandestine materials with nuclear resonance fluorescence”, Jour. Appl. Phys. **99**, 123102 (2006).